

Journal of Paleontology



CAMBRIDGE
UNIVERSITY PRESS

**Earliest known spatial competition between
stromatoporoids: evidence from the Upper Ordovician
Xiazhen Formation of South China**

Journal:	<i>Journal of Paleontology</i>
Manuscript ID	JPA-RA-2019-0027.R3
Manuscript Type:	Regular Article
Date Submitted by the Author:	n/a
Complete List of Authors:	Jeon, Juwan; NIGPAS CAS, CAS Key Laboratory of Economic Stratigraphy and Palaeogeography, Nanjing Institute of Geology and Palaeontology and Center for Excellence in Life and Palaeoenvironment; NIGPAS CAS, State Key Laboratory of Palaeobiology and Stratigraphy, Nanjing Institute of Geology and Palaeontology and Center for Excellence in Life and Palaeoenvironment; UCAS, University of Chinese Academy of Sciences Liang, Kun; NIGPAS CAS, CAS Key Laboratory of Economic Stratigraphy and Palaeogeography, Nanjing Institute of Geology and Palaeontology and Center for Excellence in Life and Palaeoenvironment; NIGPAS CAS, State Key Laboratory of Palaeobiology and Stratigraphy, Nanjing Institute of Geology and Palaeontology and Center for Excellence in Life and Palaeoenvironment Lee, Mirinae; Korea Polar Research Institute, Division of Polar Earth-System Sciences Kershaw, Stephen; Brunel University, Kingston Lane, Department of Life Sciences
Taxonomy:	other Porifera < Porifera
Broad Geologic Time:	Ordovician < Paleozoic
Detailed Geologic Time:	Upper < Ordovician

Subject area Geographic Location:	Asia (eastern)

SCHOLARONE™
Manuscripts

1 **Earliest known spatial competition between stromatoporoids:**
2 **evidence from the Upper Ordovician Xiashen Formation of South**
3 **China**

4

5 Juwan Jeon^{1, 2, 3}, Kun Liang^{1, 2*}, Mirinae Lee⁴ and Stephen Kershaw⁵

6

7 ¹CAS Key Laboratory of Economic Stratigraphy and Palaeogeography, Nanjing Institute of
8 Geology and Palaeontology and Center for Excellence in Life and Palaeoenvironment,
9 Chinese Academy of Sciences, Nanjing 210008, China10 ²State Key Laboratory of Palaeobiology and Stratigraphy, Nanjing Institute of Geology and
11 Palaeontology and Center for Excellence in Life and Palaeoenvironment, Chinese Academy of
12 Sciences, 39 East Beijing Road, Nanjing 210008, China13 ³University of Chinese Academy of Sciences (UCAS), Beijing 100049, China14 ⁴Division of Polar Earth-System Sciences, Korea Polar Research Institute, Incheon 21990,
15 Korea16 ⁵Department of Life Sciences, Brunel University, Kingston Lane, Uxbridge, UB8 3PH,
17 United Kingdom

18

19 E-mail: Jeon Juwan [jjeon@nigpas.ac.cn], Liang Kun [kliang@nigpas.ac.cn], Lee Mirinae
20 [mirinae.lee@kopri.re.kr]; Stephen Kershaw [stephen.kershaw@brunel.ac.uk]

21

22 ***Corresponding author:** Kun Liang: kliang@nigpas.ac.cn, Tel. 86-25-8328-4310

23

24 **Running Header:** Earliest known spatial competition between stromatoporoids

25

26 **Abstract.**—The earliest known interpreted spatial competition between two species of
27 stromatoporoids, *Clathrodictyon* cf. *C. mammillatum* (Schmidt, 1858) and *Labechia* sp. is
28 found in the Upper Ordovician Xiazhen Formation at Zhuzhai, South China. The interaction
29 between these taxa was initiated by settlement of *Labechia* sp. on the surface of *C.* cf. *C.*
30 *mammillatum*. Distortions of the intraskeletal elements of stromatoporoids represented by
31 abnormally large, wide cysts and thick cyst plates in *Labechia* sp. are observed, along with
32 zigzag crumpled distorted laminae and antagonistic behavior of the skeleton in *C.* cf. *C.*
33 *mammillatum*, indicating syn-vivo interactions. The growth of *Labechia* sp. was terminated
34 by the overgrowth of *C.* cf. *C. mammillatum*, possibly reflecting the ecological superiority of
35 *C.* cf. *C. mammillatum* over *Labechia* sp. The observations are interpreted as competitive
36 interaction between stromatoporoids and was most likely facultative, thus most likely
37 occurring by chance, but the interaction allows assessment of different growth behaviors of
38 the stromatoporoid species. Analysis of the interaction provides evidence to improve
39 understanding of the paleoecology and growth behaviors of early stromatoporoids.

40

41 **Introduction**

42

43 Paleozoic stromatoporoids were one of the most abundant organisms in reef complexes and
44 associated facies from the Ordovician to the Late Devonian (Kershaw, 2015; Stearn, 2015;

45 Kershaw et al., 2018). They lived in warm, shallow, tropical to subtropical marine
46 environments, exhibiting a variety of growth forms (Stock et al., 2015; Webby et al., 2015)
47 and are commonly found associated with other organisms, including many cases of
48 intergrowth with other organisms such as tabulate and rugose corals, brachiopods, bryozoans
49 and worm tubes in reef environments (e.g., Kershaw, 1987; Young and Noble, 1989; Zhen
50 and West, 1997; Lin and Webby, 1998; Nestor et al., 2010; Da Silva et al., 2011; Vinn and
51 Wilson, 2012; Vinn and Mõtus, 2014; Stearn, 2015; Lee et al., 2016; Kershaw et al., 2018).

52 Many associations between stromatoporoids and other organisms may be interpreted as
53 spatial competition with, or predation by, the associated other organisms; some cases have
54 been considered to be symbiotic interactions based on modification of the adjacent skeletal
55 structure of the host stromatoporoid (Kershaw et al., 2018). The majority of intergrowth
56 associations are known from Silurian and Devonian strata (e.g., Mori, 1970; Kershaw, 1987;
57 Young and Noble, 1989; Nestor et al., 2010; Da Silva et al., 2011; Vinn and Wilson, 2012;
58 Vinn and Mõtus, 2014; Vinn et al., 2015; Vinn, 2016a, b), with a few recorded from
59 Ordovician rocks (e.g., Lin and Webby, 1998; Lee et al., 2016).

60 These symbiotic interactions resulting from the associated organisms caused interruption
61 of stromatoporoid growth (Webby and Kershaw, 2015; Kershaw et al., 2018), which is
62 important for understanding growth control of stromatoporoids (Kershaw et al., 2018).
63 However, interactions between different stromatoporoids have rarely been described from the
64 fossil record although intergrowth between the skeletons of two or more stromatoporoids
65 frequently occurs in reefal environments (Stearn, 2015). Prosh and Stearn (1996) briefly
66 mentioned the interaction between two Devonian species of stromatoporoids and interpreted
67 their relationship as spatial competition. However, more detailed investigation of the
68 interactions between two or more stromatoporoids is required to fully verify the nature of the
69 relationship.

70 In this study, we document and interpret the inter-genera interactions between two species
71 of Late Ordovician stromatoporoid, *Clathrodictyon* Nicholson and Murie, 1878 and *Labechia*
72 Milne-Edwards and Haime, 1851 from the Upper Ordovician Xiazhen Formation at Zhuzhai,
73 Jiangxi Province, China. The aim of study is to assess the nature of the earliest known spatial
74 interaction between stromatoporoids, thus providing new information to understand the
75 paleoecology and growth behaviors of early stromatoporoids.

76

77 **Geological setting**

78

79 The Jiangshan–Changshan–Yushan (JCY) triangle region of South China is located in the
80 border area between Jiangxi and Zhejiang provinces (Fig. 1.1). The JCY triangle is a
81 representative region for studying the Ordovician System in South China (Zhang et al., 2007).
82 The Ordovician carbonate successions in the region were deposited on the Zhe-Gan Platform
83 in the northern part of the Cathaysian landmass (Chen et al., 1987; Rong and Chen, 1987;
84 Wu, 2003; Zhang et al., 2007; Zhan and Jin, 2007; Rong et al., 2010). The Upper Ordovician
85 Xiazhen Formation at Zhuzhai, Yushan County is one of the best-exposed Ordovician
86 carbonate successions in the region and is considered to be correlated to the Sanqushan and
87 Changwu formations in Jiangshan and Changshan counties (Zhang et al., 2007). The
88 stratigraphy of the 190 m thick formation has been revised on the basis of detailed
89 lithological and paleontological data (Lee et al., 2012).

90 The depositional environments of the Xiazhen Formation are interpreted as shallow-marine
91 deposits of an epicontinental sea north of the Cathaysian landmass of South China (Li et al.,
92 2004; Lee et al., 2012). Based on fossils and correlation with the Sanqushan and Changwu
93 Formation, the age of the Xiazhen Formation is estimated to be middle to late Katian (Zhang

94 et al., 2007). In addition, the finding of the graptolite *Anticostia uniformis* in the upper shale
95 member of the formation (Chen et al., 2016) indicates that the upper part of the Xiazhen
96 Formation at Zhuzhai is within the range of the *Dicellograptus complanatus* (middle Katian)
97 to *Normalograptus persculptus* (late Hirnantian) graptolite biozones (Chen et al., 2016).

98

99 **Materials and methods**

100

101 More than 400 stromatoporoid specimens were collected and examined by thin sections, but
102 only one specimen shows clear interactions between two stromatoporoids. This studied rock
103 sample is from the uppermost interval of the Xiazhen Formation, above the upper shale
104 member (arrows in Fig. 1.2, 1.3). The interval, which is characterized by limestone–shale
105 couplets in mudstone to packstone (Fig. 1.4), contains abundant patch reefs that are
106 composed of mainly dendroid clathrodictyids in a variety of orientations and the tabulate
107 corals *Agetolites*, *Catenipora*, *Heliolites* and *Plasmoporella*.

108 For a better observation of the stromatoporoid growth patterns, 20 serial sections of the
109 specimens were prepared at intervals ranging from 1.0 to 1.2 mm. The taxonomic
110 assignments of stromatoporoids follow Webby (2015b) and Nestor (2015).

111

112 *Repository and institutional abbreviation.*—All serial thin sections, used in this study are
113 deposited in Nanjing Institute of Geology and Palaeontology (NIGP), Chinese Academy of
114 Sciences, Nanjing, China as following specimen number; NIGP 169634-1–20.

115

116 **Results**

117

118 *Intergrown stromatoporoid species*.—Stromatoporoids are common sessile organisms in the
119 Xiazhen Formation. Three genera of clathrodictyids and eight genera of labechiids are
120 recorded from the formation (Jeon et al., 2018). The stromatoporoid assemblage is
121 characterized by the dominance by *Clathrodictyon*, which has the longest stratigraphic range
122 throughout the formation of the diverse stromatoporoid fauna (Jeon et al., 2018). The two
123 stromatoporoid species involved in the interaction are identified as *Clathrodictyon* cf. *C.*
124 *mammillatum* (Schmidt, 1858) and *Labechia* sp.

125 *Clathrodictyon* is characterized by its continuous laminae, which are commonly irregularly
126 wrinkled, with short funnel-shaped, rod-like or oblique pillars (Nestor, 2015). The
127 *Clathrodictyon* species involved in the syn-vivo interaction is identified as *Clathrodictyon* cf.
128 *C. mammillatum* (Schmidt, 1858; Fig. 2.1, 2.2). Based on longitudinal sections (Fig. 2.2), its
129 laminae are well developed and continuous, showing slight undulations between rare short
130 rod-like pillars. Lamina thickness ranges from 0.10 to 0.32 mm (mean = 0.19 mm, n = 50),
131 and there are commonly 9 to 12 laminae in a vertical thickness of 2 mm (Fig. 2.2). Mamelon
132 columns are common, although partially dissolved due to diagenesis. Pillars are short, rod-
133 like and restricted to interlaminar spaces, forming irregular galleries. This species is also
134 reported from the Sanjushan Formation at Yushan (Lin and Webby, 1988).

135 The other stromatoporoid species is characterized by well-developed upwardly convex cyst
136 plates and pillars, which are diagnostic of labechiids (Webby, 2015b). Most cyst plates have
137 an irregular outline in transverse view (Fig. 2.3), and some are moderately to highly convex
138 in vertical section (Fig. 2.4). In transverse view, pillars are ellipsoidal to circular in shape,
139 and most are preserved hollow and flanged, locally solid, with a thickness of 0.15–0.36 mm
140 (mean = 0.24 mm, n = 45; Fig. 2.3). In longitudinal section, stout, round pillars are developed
141 intermittently (Fig. 2.4). In this study the taxon is reasonably identified as *Labechia* sp. from
142 the direct evidence of the morphological features, including convex cyst plates with round

143 and stout pillars (Fig. 2.3, 2.4), which are characteristic of *Labechia* rather than *Labechiella*,
144 and different from any other labechiid genera.

145 *Ecological interactions between stromatoporoids.*—In the Xiazhen Formation,
146 *Clathrodictyon* and *Labechia* co-occur in four of the total 18 stromatoporoid-bearing
147 intervals (Jeon et al., 2018), but their intergrowth is recognized only from the uppermost
148 interval of the formation, which is interpreted as a patch reef environment. A single specimen
149 (NIGP 169634) shows that the beginning of the intergrowth started with the settlement of
150 *Labechia* sp. on the growth surface of *Clathrodictyon* cf. *C. mammillatum* (Figs. 2.4, 3, 4).
151 Ecological interactions can be judged from the thicker-than-normal growth of the cyst plates
152 of *Labechia* sp. (Figs. 2.4, 3.1–3.3, 4.6–4.8) and the highly distorted character of the
153 interaction between the two stromatoporoids (Figs. 2.4, 3, 4). Subsequently, larger-sized,
154 irregularly shaped cysts, which are indicative of rapid growth after initial settlement,
155 appeared in the basal portion of *Labechia* sp. Such cyst malformations (abnormally thick cyst
156 plates and large, irregular cysts) are commonly observed not only in the initial portion of the
157 skeleton, but also in subsequent growth stages (Figs. 2.4, 3, 4).

158 Distorted skeletal structure in *Clathrodictyon* cf. *C. mammillatum* is commonly observed
159 where its skeleton is in contact with *Labechia* sp. and also possibly by sediment interruptions
160 (Figs. 2.4, 3, 4). The distortion in *C. cf. C. mammillatum* appears to be weaker than that in
161 *Labechia* sp. The abnormal development of *C. cf. C. mammillatum* is manifest as zigzag
162 crumpled distorted structure (Figs. 2.4, 3.3). It is necessary to note that even within one
163 stromatoporoid specimen, the structure can vary significantly in relation to disturbing
164 influences during its growth. In some instances, the laminae of *C. cf. C. mammillatum* occupy
165 the cyst interspaces of *Labechia* sp., and its interskeletal structure exhibits distorted growth,
166 which is considered to represent antagonistic behavior (aggressive and passive reactions;
167 Figs. 2.4, 3.2, 4.7–4.8).

168 The occurrence of abnormal growth in both stromatoporoids indicates that their
169 intergrowth occurred while both organisms were alive. Finally, their intergrowth ceased
170 because *Clathrodictyon* cf. *C. mammillatum* overgrew *Labechia* sp. (Figs. 3, 4). It is apparent
171 that the *C. cf. C. mammillatum* individual lived longer than the *Labechia* sp. individual and
172 may have ultimately had a faster growth rate.

173 In addition to the interaction with *Labechia* sp., *Clathrodictyon* cf. *C. mammillatum* served
174 as a host for various endobionts including the tabulate coral *Bajgolia* and the solitary rugose
175 corals *Tryplasma* and *Streptelasma* (Fig. 5). However, there was no distortion of skeletal
176 elements in *C. cf. C. mammillatum*, suggesting that the growth of the stromatoporoid was not
177 greatly affected by the coral intergrowth, or that the stromatoporoid grew around pre-existing
178 coral skeletons.

179

180 Discussion

181

182 *Earliest known stromatoporoid spatial competition.*—Intergrowth associations have
183 previously been interpreted as an adaptation to seek shelter from adverse environmental
184 conditions (e.g., competition, predation or depositional environments; Webby and Kershaw,
185 2015; Kershaw et al., 2018) or enhanced substrate stability (Vinn and Mötus, 2014; Lee et al.,
186 2016; Vinn et al., 2017). It has been proposed that stromatoporoids with well-developed
187 laminae probably provided more favourable substrates for the settlement of tabulate corals
188 than other stromatoporoids (Mori, 1970). This phenomenon applies particularly to Ordovician
189 stromatoporoids, in which intergrowth commonly occurs between corals and stromatoporoids
190 possessing well-developed laminae, such as the clathrodictyids (e.g., Lin and Webby, 1988;
191 Lee et al., 2016). In this study, *Clathrodictyon* cf. *C. mammillatum* which possesses well-

192 developed mamelon columns possibly provided a suitable substrate for the growth of
193 *Labechia* sp. The serial sections demonstrate a competitive interaction between
194 *Clathrodictyon* cf. *C. mammillatum* and *Labechia* sp, and that both stromatoporoids were
195 significantly affected, as judged by the distorted skeletal structures. We speculate that the
196 settlement of *Labechia* sp. caused a reduction in the feeding surface of *C. cf. C.*
197 *mammillatum*. Therefore, the distortion (Figs. 2.4, 3, 4) and consequent change in growth
198 habit produced distorted structures indicative of soft tissue reaction of *C. cf. C. mammillatum*
199 (Fig. 6.1–6.3). In contrast, abundant apparent endobionts *Bajgolia* are associated with
200 *Clathrodictyon*, especially around mamelon columns, but no distortion of skeletal structures
201 is observed in *C. cf. C. mammillatum* in these cases (Fig. 5.3, 5.4). In addition, densely
202 spaced *Bajgolia* are commonly observed to occupy a relatively large area of the centre of the
203 mamelon columns of clathrodictyids (Lee et al., 2016, figs. 2h, 3c, 6). It is obvious that
204 interaction with *Bajgolia* was not critical to the feeding of *C. cf. C. mammillatum*, whereas
205 the settlement of *Labechia* sp. significantly affected the skeleton of *C. cf. C. mammillatum*. In
206 the same horizon, not only *Bajgolia* also other tabulate corals including *Heliolites* and
207 solitary rugose corals *Streptelasma* and *Tryplasma* occur. The solitary rugose corals have
208 been reported and interpreted as endobionts in species of *Clathrodictyon* based on
209 longitudinal sections (Lee et al., 2016, fig. 2; Fig. 5). It is noteworthy that none of the
210 *Clathrodictyon* skeletons exhibit malformation from their coral endobionts. Therefore, this
211 difference suggests that the modifications of *Clathrodictyon* cf. *C. mammillatum* and
212 *Labechia* sp. are due to spatial competition between each other, rather than being an example
213 of commensalism or parasitism, as reported from the endobiotic corals and other organisms
214 (e.g., Lee et al., 2016; Vinn et al., 2015, 2017; Zapalski and Hubert, 2010). This is the earliest
215 known interpreted spatial competition between stromatoporoids, occurring in the uppermost
216 interval of Xiazhen Formation at Zhuzhai, South China, within the range of the

217 *Dicellograptus complanatus* (middle Katian) to *Normalograptus persculptus* (late Hirnantian)
218 graptolite biozones (Chen et al., 2016).

219 Of the two stromatoporoids involved in the intergrowth, the skeleton of *Labechia* sp.
220 possesses irregularly spaced, large cysts different from normal forms, whereas the skeleton of
221 *C. cf. C. mammillatum* exhibits rather regularly spaced laminae, similar to the other skeletons
222 of the species from this interval except for showing crumpled, distorted skeletal structure.
223 This difference is possibly related to the different growth rates of the two species, as *C. cf. C.*
224 *mammillatum* is likely to have grown faster than *Labechia* sp.

225 Very few previous studies concern the intergrowth between different stromatoporoids. The
226 association between *Gerronostroma septentrionalis* Prosh and Stearn, 1996 and
227 *Stromatopora polaris* (Stearn, 1983) was reported from Lower Devonian (Emsian) of Arctic
228 Canada and their relationship is described as competitive (Prosh and Stearn, 1996). Based on
229 the illustration, it is noteworthy that none of the distorted skeletal structures occurred by the
230 interfingering contact (Prosh and Stearn, 1996, pl. 4, fig. 4), which is different from the
231 present study. As little is known about the intergrowth between different stromatoporoids,
232 further studies on other formations are necessary, in order to understand the growth behaviors
233 of stromatoporoids.

234 *Paleoecological implications.*—Both *Clathrodictyon* and *Labechia* are widely distributed
235 in Late Ordovician sedimentary sequences (Nestor and Webby, 2013; Stock et al., 2015). The
236 labechiids appeared in the late Early Ordovician (Li et al., 2017) and initially diversified in
237 the late Middle Ordovician (Webby, 2004; Nestor and Webby, 2013; Stock et al., 2015;
238 Webby, 2015a), which was earlier than the clathrodictyids. The clathrodictyids, however,
239 spread rapidly and achieved a circum-equatorial distribution in the Late Ordovician (Nestor
240 and Webby, 2013). Later, they became a major cosmopolitan group after a rapid radiation in
241 the Silurian, which was crucial to the evolution of Paleozoic stromatoporoids (Nestor, 1997).

242 A recent study on the intergrowth between stromatoporoids and the tabulate coral *Bajgolia*
243 revealed that only two clathrodictyid genera (*Clathrodictyon* and *Ecclimadictyon*) contained
244 various endobionts such as tetradiids, tabulate corals and solitary rugose corals (Lee et al.,
245 2016). In addition, *Clathrodictyon* is the most abundant stromatoporoid genus in the Xiazhen
246 Formation, occupying a long stratigraphic distribution and a wide range of lithofacies (Jeon et
247 al., 2018). The long stratigraphic range of *Clathrodictyon* in the formation is a potential
248 indication that clathrodictyids, especially *Clathrodictyon*, had broader ecological plasticity
249 and more flexible growth strategies than did labechiids (Jeon et al., 2018). Correspondingly,
250 the spatial competition between *Clathrodictyon* cf. *C. mammillatum* and *Labechia* sp.
251 provides direct evidence that *Clathrodictyon* could outcompete *Labechia* as a result of its
252 flexible growth behaviors (Fig. 6).

253 Compared with the coral-stromatoporoid association, the interaction between
254 *Clathrodictyon* and *Labechia* occurs more rarely in the formation. Their relationship seems to
255 be facultative rather than obligatory, which is similar to the coral-stromatoporoid and
256 tabulate-rugose corals associations (Lee et al., 2016; Vinn et al., 2017). Due to lack of clear
257 evidence, the nature of the relationship between various endobionts and the hosting
258 stromatoporoids is difficult to explore, as very often there are no skeletal distortions among
259 the organisms. The intergrowth between corals and stromatoporoids was commonly
260 interpreted to be commensalism, as their growth seems unaffected (e.g., Mori, 1970;
261 Kershaw, 1987; Vinn, 2016a), whereas tubeworm endobionts, including *Cornulites*,
262 *Streptindytes*, and *Torquaysalpinx* seem to be more complex to evaluate (Vinn, 2016b).
263 Based on the downbending-curved laminae of stromatoporoids in the vicinity of the symbiont
264 tube, the *Torquaysalpinx*-stromatoporoid relationship is interpreted to be parasitism (Zapalski
265 and Hubert, 2011). Downwardly or upwardly curved laminae near the contact with the
266 endobionts has been considered as a criterion to judge whether it is positive or negative to the

267 hosting stromatoporoids (Kershaw, 1987, 2013; Young and Noble, 1989; Lee et al., 2016).
268 This study shows that evaluation of distorted structures in the intergrown organisms are also
269 important for analysing their ecological relationship. In addition, the fact that spatial
270 competition between different stromatoporoids in the reefs appeared as early as in the Late
271 Ordovician suggests that spatial competition, which has been studied extensively in modern
272 marine communities, deserves greater emphasis in the understanding of Paleozoic reef
273 ecosystems.

274

275 **Conclusions**

276

277 We report the earliest known spatial competition between two species of stromatoporoids,
278 *Clathrodictyon* cf. *C. mammillatum* and *Labechia* sp., from the Upper Ordovician Xiazhen
279 Formation at Zhuzhai, South China. *Labechia* sp. exhibits large-sized and irregularly shaped
280 cysts, indicative of rapid growth after initial settlement on the surface of *C.* cf. *C.*
281 *mammillatum*. Alteration of the growth pattern of *C.* cf. *C. mammillatum* to produce
282 crumpled distorted skeletal structure occurs during the interaction with *Labechia* sp.
283 Intergrowth between *C.* cf. *C. mammillatum* and tabulate and solitary rugose corals suggests
284 that corals did not significantly affect the growth of stromatoporoids and thus did not cause
285 distortion of the stromatoporoid skeleton. Obviously distorted skeletal elements are present at
286 the physical contact between the different stromatoporoids, indicating spatial competition
287 between the organisms. This study of competitive interaction between stromatoporoids
288 increases our understanding of the paleoecology and growth behaviors of early
289 stromatoporoids. The spatial competition between *Clathrodictyon* cf. *C. mammillatum* and

290 *Labechia* sp. provides direct evidence that species of *Clathrodictyon* have more flexible
291 growth behaviours than those of *Labechia*.

292

293 **Acknowledgments**

294

295 Funds from the Chinese Academy of Sciences (XDB26000000) and the National Science
296 Foundation of China (Grant No. 41402013 and J1210006) to KL, Korea Polar Research
297 Institute to ML (PE19160) and the Chinese Academy of Sciences (CAS) ‘One Belt and One
298 Road’ Master Fellowship Program and a CAS President’s International Fellowship Initiative
299 (PIFI) to JJ are acknowledged. We appreciate the journal editor, B. Hunda and J. Botting for
300 constructive reviews. We thank O. Vinn and an anonymous reviewer for providing valuable
301 comments. We are also grateful to Y.D. Zhang, H. Park, and J. Park for their assistance on
302 the manuscript. We deeply appreciate the warm hospitality and assistance during field work
303 of the residents of Zhuzhai village. This paper is a contribution to IGCP 653 ‘The Onset of
304 the Great Ordovician Biodiversification Event’.

305

306 **References**

307

308 Chen, X., Rong, J.Y., Qiu, J.Y., Han, N.R., Li, L.Z., and Li, S. J., 1987, Preliminary
309 stratigraphy, sedimentologic and environmental investigation of Zhuzhai section: Journal
310 of Stratigraphy, v. 11, p. 23–34. [In Chinese with English abstract]

311 Chen, Z.Y., Kim, M.H., Choh, S.J., Lee, D.-J., and Chen, X., 2016, Discovery of *Anticostia*
312 *uniformis* from the Xiazhen Formation at Zhuzhai, South China and its stratigraphic
313 implication: Palaeoworld, v. 25, p. 356–361.

- 314 Da Silva, A.-C., Kershaw, S., and Boulvain, F., 2011, Stromatoporoid palaeoecology in the
315 Frasnian (Upper Devonian) Belgian platform, and its applications in interpretation of
316 carbonate platform of carbonate platform environments: *Palaeontology*, v. 54, p. 883–905.
- 317 Jeon, J., Liang, K., Park J., Choh, S.-J., and Lee, D.-J., 2018, Late Ordovician
318 stromatoporoids from the Xiazhen Formation of South China: paleoecological and
319 paleogeographical implications: *Geological Journal*, published online 14 December 2018,
320 p. 1–13. <https://doi.org/10.1002/gj.3401>
- 321 Kershaw, S., 1987, Stromatoporoid–coral intergrowths in a Silurian biostrome: *Lethaia*, v. 20,
322 p. 371–382.
- 323 Kershaw, S., 2015, Paleoecology of the Paleozoic Stromatoporoidea, *in* Selden, P.A., ed.,
324 *Treatise on Invertebrate Paleontology*, Part E (Revised), Porifera, Vol. 4–5: The University
325 of Kansas Paleontological Institute, Lawrence, Kansas, p. 631–651.
- 326 Kershaw, S., Munnecke, A., and Jarochovska, E., 2018, Understanding Palaeozoic
327 stromatoporoid growth: *Earth-Science Reviews*, v. 187, p. 53–76.
- 328 Lee, D.-C., Park, J., Woo, J., Kwon, Y.K., Lee, J.-G., Guan, L., Sun, N., Lee, S.-B., Liang K.,
329 Liu, L., Rhee, C.-W., Choh, S.-J., Kim, B.-S., and Lee, D.-J., 2012, Revised stratigraphy of
330 the Xiazhen Formation (Upper Ordovician) at Zhuzhai, South China, based on
331 palaeontological and lithological data: *Alcheringa*, v. 36, p. 387–404.
- 332 Lee, M., Elias, R.J., Choh, S.-J., and Lee, D.-J., 2016, Insight from early coral–
333 stromatoporoid intergrowth, Late Ordovician of China: *Palaeogeography*,
334 *Palaeoclimatology*, *Palaeoecology*, v. 463, p. 192–204.
- 335 Li, Q., Li, Y., and Kiessling, W., 2017, The oldest labechiid stromatoporoids from
336 intraskeletal crypts in lithistid sponge–*Calathium* reefs: *Lethaia*, v. 50, p. 140–148.

- 337 Li, Y., Kershaw, S., and Mu, X., 2004, Ordovician reef systems and settings in South China
338 before the Late Ordovician mass extinction: *Palaeogeography, Palaeoclimatology,*
339 *Palaeoecology*, v. 205, p. 235–254.
- 340 Lin, B.-Y., and Webby, B.D., 1988, Clathrodictyid stromatoporoids from the Ordovician of
341 China: *Alcheringa*, v. 12, p. 233–247.
- 342 Milne-Edwards, H., and Haime, J., 1851, *Monographie des Polypiers fossils des Terrainés*
343 *Paleozoïques, précédée d'un tableau general de la classification des Polypes: Archives du*
344 *Muséum d'Histoire naturelle de Paris* 5, 502 p.
- 345 Mori, K., 1970, Stromatoporoids from the Silurian of Gotland, Part 2: Stockholm
346 *Contributions in Geology* 22, Stockholm, 152 p.
- 347 Nestor, H., 1997, Evolutionary history of the single-layered, laminate, clathrodictyid
348 stromatoporoids: *Boletín de la Real Sociedad Española de Historia Natural, Sección*
349 *Geológica*, v. 91, p. 319–328.
- 350 Nestor, H., 2015. Clathrodictyida: Systematic descriptions, *in* Selden, P.A., ed., *Treatise on*
351 *Invertebrate Paleontology, Part E (Revised), Porifera, Vol. 4–5: The University of Kansas*
352 *Paleontological Institute, Lawrence, Kansas*, p. 755–768.
- 353 Nestor, H., and Webby, B.D., 2013, Biogeography of the Ordovician and Silurian
354 Stromatoporoidea, *in* Harper, D.A.T., and Servais, T. eds., *Early Palaeozoic biogeography*
355 *and palaeogeography: Geological Society of London, Memoir* 38, London, p. 67–79.
- 356 Nestor, H., Copper, P., and Stock, C., 2010, Late Ordovician and Early Silurian
357 Stromatoporoid Sponges from Anticosti Island, Eastern Canada: Crossing the O/S Mass
358 Extinction Boundary: *National Research Council Research Press, Ottawa, Canada*, 152 p.
- 359 Nicholson, H.A., and Murie J., 1878, On the minute structure of *Stromatopora* and its allies:
360 *Zoological Journal of the Linnean Society*, v. 14, p. 187–246.

- 361 Prosh, E.C., and Stearn, C.W., 1996, Stromatoporoids from the Emsian (Lower Devonian) of
362 Arctic Canada: *Bulletins of American Paleontology*, v. 109, p. 1–66.
- 363 Rong, J.Y., and Chen, X., 1987, Faunal differentiation, biofacies and lithofacies patterns of
364 the Late Ordovician (Ashgillian) in South China: *Acta Palaeontologica Sinica*, v. 26, p.
365 507–535. [In Chinese with English abstract]
- 366 Rong, J.Y., Zhan, R.B., Xu, H.G., Huang, B., and Yu, G.H., 2010, Expansion of the
367 Cathaysian Oldland through the Ordovician-Silurian transition: emerging evidence and
368 possible dynamics: *Science China, Earth Science*, v. 53, p. 1–17.
- 369 Schmidt, F., 1858, Untersuchungen über die Silurische Formation von Ehstland, Nord-
370 Livland und Oesel: *Archiv für die Naturkunde Liv-, Esth- und Kurlands*, erster serie, Bd.
371 II, 248 p.
- 372 Stearn, C.W., 1983, Stromatoporoids from the Blue Fiord Formation (Lower Devonian) of
373 Ellesmere Island, Arctic Canada: *Journal of Paleontology*, v. 57, p. 539–559.
- 374 Stearn, C.W., 2015, Internal morphology of the Paleozoic Stromatoporoidea, *in* Selden, P.A.
375 ed., *Treatise on Invertebrate Paleontology, Part E (Revised), Porifera, Vol. 4–5: The*
376 *University of Kansas Paleontological Institute, Lawrence, Kansas*, p. 487–520.
- 377 Stock, C.W., Nestor, H., and Webby, B.D., 2015, Paleobiogeography of the Paleozoic
378 Stromatoporoidea, *in* Selden, P.A. ed., *Treatise on Invertebrate Paleontology, Part E*
379 *(Revised), Porifera, Vol. 4–5: The University of Kansas Paleontological Institute,*
380 *Lawrence, Kansas*, p. 653–689.
- 381 Vinn, O., 2016a, Symbiotic endobionts in Palaeozoic stromatoporoids: *Palaeogeography,*
382 *Palaeoclimatology, Palaeoecology*, v. 453, p. 146–153.
- 383 Vinn, O., 2016b, Tentaculitoid tubeworms as endobiotic symbionts of Paleozoic corals and
384 sponges. *Palaios*, v. 31, p. 440–446

- 385 Vinn, O., and Mõtus, M.-A., 2014, Endobiotic Rugosan symbionts in stromatoporoids from
386 the Sheinwoodian (Silurian) of Baltica: PLoS ONE 9: e90197.
387 <http://dx.doi.org/10.1371/journal.pone.0090197>.
- 388 Vinn, O., and Wilson, M.A., 2012, Epi- and endobionts on the late Silurian (early Pridoli)
389 stromatoporoids from Saaremaa Island, Estonia: *Annales Societatis Geologorum Poloniae*,
390 v. 82, p. 195–200.
- 391 Vinn, O., Toom, U., and Mõtus, M.-A., 2015, Earliest known rugosan-stromatopoid
392 symbiosis from the Llandovery of Estonia (Baltica): *Palaeogeography, Palaeoclimatology,*
393 *Palaeoecology*, v. 431, p. 1–5.
- 394 Vinn, O., Liang, K., and Toom, U., 2017, Endobiotic rugose coral symbionts in Silurian
395 tabulate corals from Estonia (Baltica): *Palaios*, v. 32, p. 158–165.
- 396 Webby, B.D., 2004, Stromatoporoids, *in* Webby, B. D., Paris, F., Droser, M. L., and Percival,
397 I. G., eds., *The Great Ordovician Biodiversification Event*: Columbia University Press,
398 New York, p. 112–118.
- 399 Webby, B.D., 2015a, Early evolution of the Paleozoic Stromatoporoidea, *in* Selden, P.A. ed.,
400 *Treatise on Invertebrate Paleontology, Part E (Revised), Porifera, Vol. 4–5: The University*
401 *of Kansas Paleontological Institute, Lawrence, Kansas*, p. 575–592.
- 402 Webby, B.D., 2015b, Labechiida: Systematic descriptions, *in* Selden, P.A. ed., *Treatise on*
403 *Invertebrate Paleontology, Part E (Revised), Porifera, Vol. 4–5: The University of Kansas*
404 *Paleontological Institute, Lawrence, Kansas*, p. 709–754.
- 405 Webby, B.D., and Kershaw, S., 2015, External morphology of the Paleozoic
406 Stromatoporoidea: Shapes and growth habits, *in* Selden, P.A. ed., *Treatise on Invertebrate*
407 *Paleontology, Part E (Revised), Porifera, Vol. 4–5: The University of Kansas*
408 *Paleontological Institute, Lawrence, Kansas*, p. 417–486.

- 409 Webby, B.D., Stearn, C.W., and Nestor, H., 2015, Biostratigraphy of the Paleozoic
410 Stromatoporoidea, *in* Selden P.A., ed., Treatise on Invertebrate Paleontology, Part E
411 (Revised), Porifera, Vol. 4–5: The University of Kansas Paleontological Institute,
412 Lawrence, Kansas, p. 613–630.
- 413 Wu, H., 2003, Tectonopalaogeographic analysis of the geologic problems related to
414 ophiolitic belt in northeastern Jiangxi Province: *Journal of Palaeogeography*, v. 5, p. 328–
415 342. [In Chinese with English abstract]
- 416 Young, G.A., and Noble, J.P.A., 1989, Variation and growth in syringoporid symbiont
417 species in stromatoporoids from the Silurian of eastern Canada: *Australasian Association*
418 *of Palaeontologists Memoir*, v. 8, p. 91–98.
- 419 Zapalski, M.K., and Hubert, B.L., 2011, First fossil record of parasitism in Devonian
420 calcareous sponges (stromatoporoids): *Parasitology*, v. 138, p. 132–138.
- 421 Zhan, R.B., and Jin, J.S., 2007, Ordovician–Early Silurian (Llandovery) Stratigraphy and
422 Palaeontology of the Upper Yangtze Platform, South China: Science Press, Beijing, 169 p.
- 423 Zhang, Y.D., Chen, X., Yu, G.H., Dan, G.D., and Liu, X., 2007, Ordovician and Silurian
424 rocks of northwest Zhejiang and northeast Jiangxi provinces, SE China: University of
425 Science and Technology of China Press, Hefei, 189 p.
- 426 Zhen, Y.-Y., and West, R.R., 1997, Symbionts in a stromatoporoid–chaetetid association
427 from the Middle Devonian Burdekin Basin, north Queensland. *Alcheringa*, v. 21, p. 271–
428 280.

429

430 **FIGURE CAPTIONS**

431

432 **Figure 1. (1)** Map of China and enlargement of the location of the border area between
433 Jiangxi and Zhejiang provinces. **(2)** Geological map of the Xiazhen Formation near the town

434 of Zhuzhai. The locality from which the specimen NIGP169634 was collected is indicated by
435 the white arrow. **(3)** Stratigraphic columns of the upper part of the Xiazhen Formation; S =
436 shale, M = mudstone, W= wackestone, P = packstone, G = grainstone, F= floatstone. All
437 figure parts are modified after Lee et al. (2012). **(4)** Field photograph of outcrop showing
438 limestone–shale couplets in mudstone to packstone. Pen for scale is 12.5 cm in length.

439

440 **Figure 2. (1–3)** Thin section photomicrographs showing normal skeletal elements, NIGP
441 169634-4. **(1)** Transverse view of *Clathrodictyon* cf. *C. mammillatum* showing small circular
442 to elliptical pillars. **(2)** Longitudinal view of *C. cf. C. mammillatum* characterized by
443 continuous and slightly undulating laminae. **(3)** Transverse view of *Labechia* sp.
444 characterized by well-developed flanged and hollow pillars with ellipsoidal to circular
445 shapes. **(4)** Vertical view of the relationship between two species of stromatoporoids. Note
446 short, stout and round pillars of *Labechia* sp. in the vertical view. Note large-sized and
447 irregular-shaped cysts of *Labechia* sp. (black arrows), distortions of *C. cf. C. mammillatum*
448 (white arrow) within the cyst interspaces of *Labechia* sp., and crumpled laminae of *C. cf. C.*
449 *mammillatum* (yellow arrow), NIGP 169634-18.

450

451 **Figure 3.** Typical distorted structures of *Clathrodictyon* cf. *C. mammillatum* and *Labechia*
452 sp. during their interactions with schematic drawings. **(1)** Abnormal large cyst of *Labechia*
453 sp. (black arrow) and distorted laminae of zigzag-crumpled shapes in *C. cf. C. mammillatum*,
454 by the settlement of *Labechia* sp. (right yellow arrow), and also possibly by sediment
455 interruption (left yellow arrow), NIGP 169634-14. **(2)** Enlarged photograph of the rectangular
456 area in (1). Note antagonistic behavior indicated by the distorted laminae of *C. cf. C.*
457 *mammillatum* (white arrow) in the cyst interspaces of *Labechia* sp., and abnormal large cysts
458 of *Labechia* sp. (black arrow) near their physical contacts. **(3)** Enlarged photograph of the

459 rectangular areas in (1) showing the physical contact between *C. cf. C. mammillatum* and
 460 *Labechia* sp. Skeletal malformation of *Labechia* sp. is manifest by uneven-thickened cyst
 461 plate and abnormal large cysts (black arrows), and zigzag crumpled laminae (yellow arrow)
 462 in *C. cf. C. mammillatum* near the physical contacts of the two stromatoporoids. **(4–9)**
 463 Schematic drawing to illustrate the process of ecological interactions between two
 464 stromatoporoids in (1).

465

466 **Figure 4. (1–5)** Transverse serial sections showing distorted skeletal elements in *Labechia*
 467 sp. and *C. cf. C. mammillatum* during their ecological interactions, each interval ranging from
 468 1.0 to 1.2 mm, respectively, exhibiting upward growth of the studied specimen, NIGP
 469 169634-8–12. **(6)** Enlargement of the left rectangular area in (2). **(7)** Enlargement of the right
 470 rectangular area in (2). **(8)** Enlargement of the right rectangular area in (3). Space occupation
 471 of the laminae of *C. cf. C. mammillatum* is reflected by their skeletal distortions (white
 472 arrows in 7 and 8) in the cyst interspaces of *Labechia* sp. Large-sized and irregular-shaped
 473 cysts of *Labechia* sp. are indicated by black arrows, while crumpled laminae of *C. cf. C.*
 474 *mammillatum* are indicated by yellow arrows.

475

476 **Figure 5.** Thin section photographs of coral endobionts within the skeleton of *Clathrodictyon*
 477 cf. *C. mammillatum*. **(1)** Oblique-cut of three solitary rugose coral *Tryplasma* (white arrows)
 478 and a solitary rugose coral *Streptelasma* (black arrow) surrounded by *C. cf. C. mammillatum*,
 479 NIGP 169634-8. **(2)** Two solitary rugose coral *Tryplasma* (white arrows) near the mamelon
 480 column of *C. cf. C. mammillatum*, NIGP 169634-11. **(3–4)** Transverse views of mamelon
 481 columns of *C. cf. C. mammillatum* and the neighboring endobiont tabulate coral *Bajgolia*
 482 (yellow arrows). Note that no distortion of *C. cf. C. mammillatum* is observed near the
 483 contacts with diverse endobionts, NIGP 169634-7, 6, respectively.

484

485 **Figure 6.** Schematic drawing to show the process of ecological interactions between two
486 stromatoporoids. **(1)** Settlement of *Labechia* sp. on the growth surface of *Clathrodictyon*; **(2)**
487 With the growth of *Labechia* sp., distorted skeleton of *C. cf. C. mammillatum* appears; **(3)**
488 *Labechia* sp. is overgrown by *C. cf. C. mammillatum*; **(4)** Schematic drawing to illustrate the
489 vertical view of *Clathrodictyon* and its endobionts including *Labechia* sp., rugose and
490 tabulate corals.

For Review Only

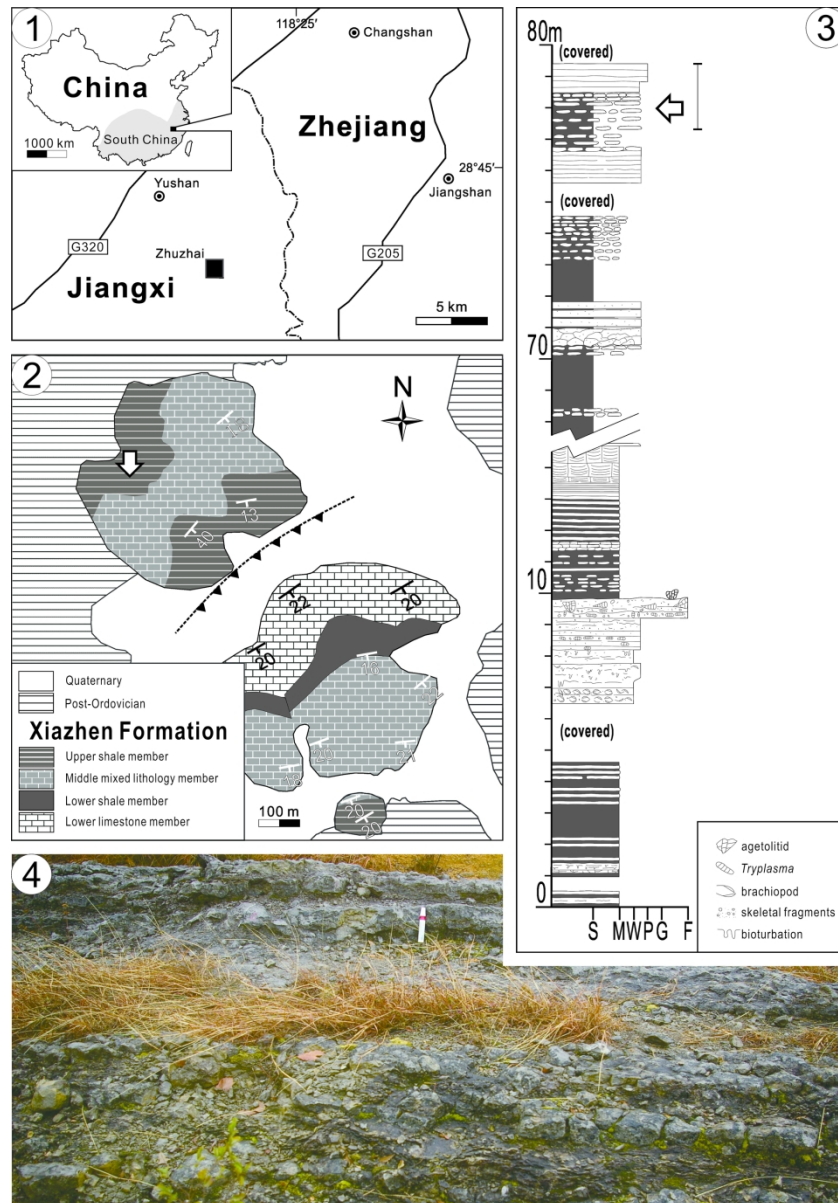


Figure 1. (1) Map of China and enlargement of the location of the border area between Jiangxi and Zhejiang provinces. (2) Geological map of the Xiazhen Formation near the town of Zhuzhai. The locality from which the specimen NIGP169634 was collected is indicated by the white arrow. (3) Stratigraphic columns of the upper part of the Xiazhen Formation; S = shale, M = mudstone, W = wackestone, P = packstone, G = grainstone, F = floatstone. All figure parts are modified after Lee et al. (2012). (4) Field photograph of outcrop showing limestone–shale couplets in mudstone to packstone. Pen for scale is 12.5 cm in length.

180x258mm (300 x 300 DPI)

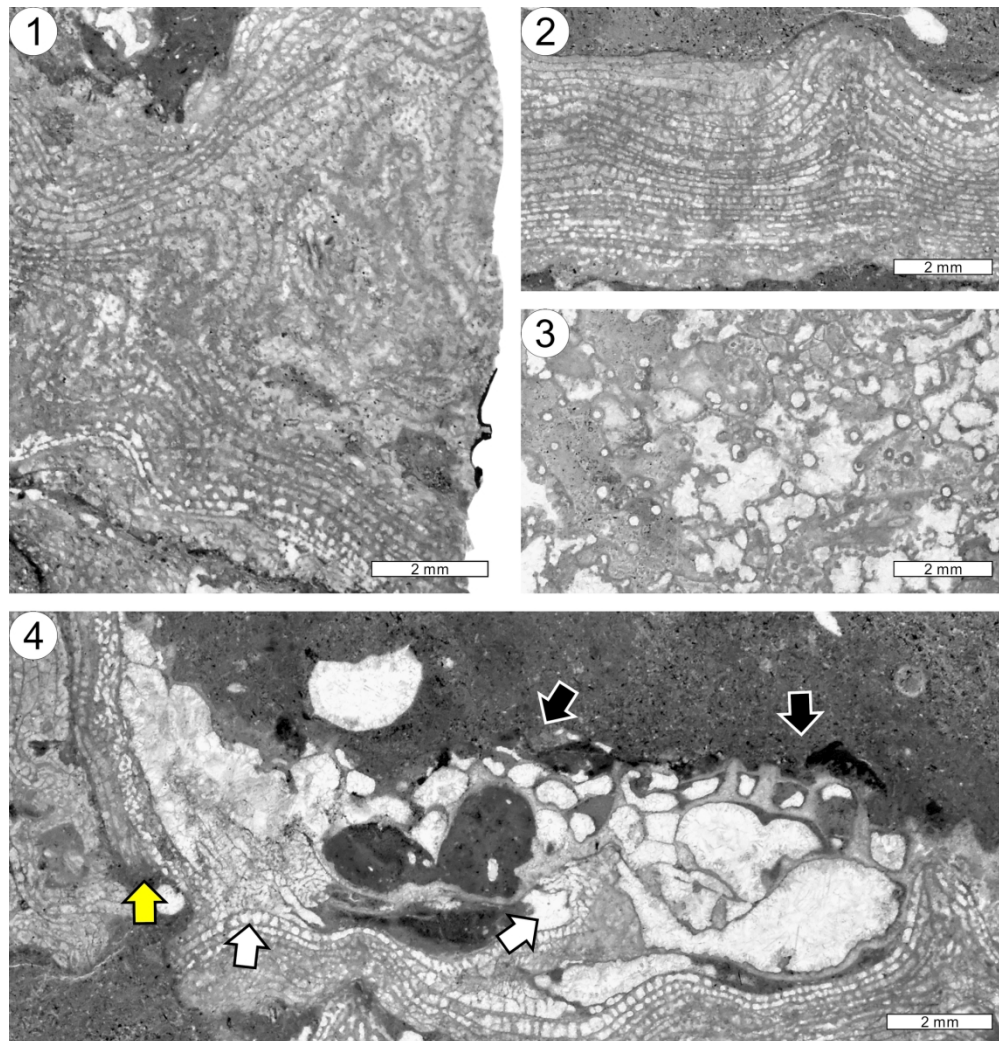


Figure 2. (1–3) Thin section photomicrographs showing normal skeletal elements, NIGP 169634–4. (1) Transverse view of *Clathrodictyon* cf. *C. mammillatum* showing small circular to elliptical pillars. (2) Longitudinal view of *C. cf. C. mammillatum* characterized by continuous and slightly undulating laminae. (3) Transverse view of *Labechia* sp. characterized by well-developed flanged and hollow pillars with ellipsoidal to circular shapes. (4) Vertical view of the relationship between two species of stromatoporoids. Note short, stout and round pillars of *Labechia* sp. in the vertical view. Note large-sized and irregular-shaped cysts of *Labechia* sp. (black arrows), distortions of *C. cf. C. mammillatum* (white arrow) within the cyst interspaces of *Labechia* sp., and crumpled laminae of *C. cf. C. mammillatum* (yellow arrows), NIGP 169634–18.

180x186mm (300 x 300 DPI)

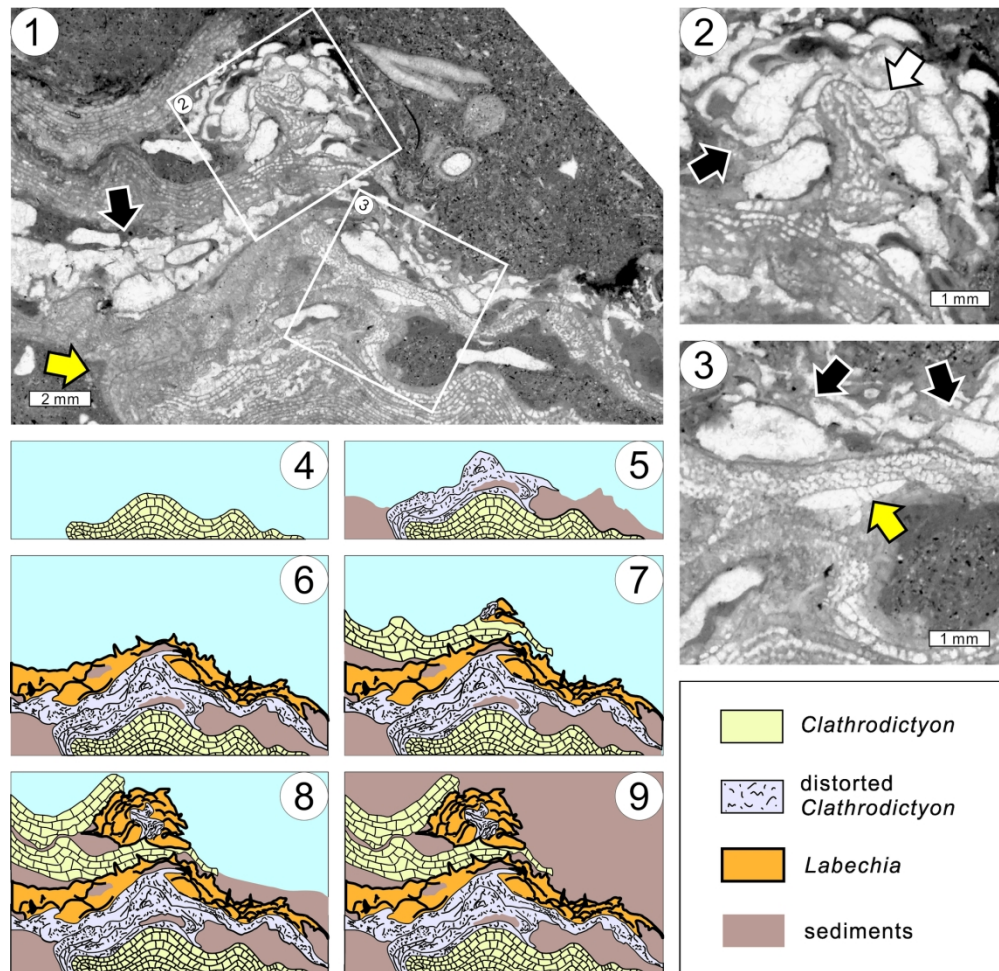


Figure 3. Typical distorted structures of *Clathrodictyon* cf. *C. mammillatum* and *Labechia* sp. during their interactions with schematic drawings. (1) Abnormal large cyst of *Labechia* sp. (black arrow) and distorted laminae of zigzag-crumpled shapes in *C. cf. C. mammillatum*, by the settlement of *Labechia* sp. (right yellow arrow), and also possibly by sediment interruption (left yellow arrow), NIGP 169634-14. (2) Enlarged photograph of the rectangular area in (1). Note antagonistic behavior indicated by the distorted laminae of *C. cf. C. mammillatum* (white arrow) in the cyst interspaces of *Labechia* sp., and abnormal large cysts of *Labechia* sp. (black arrow) near their physical contacts. (3) Enlarged photograph of the rectangular areas in (1) showing the physical contact between *C. cf. C. mammillatum* and *Labechia* sp. Skeletal malformation of *Labechia* sp. is manifest by uneven-thickened cyst plate and abnormal large cysts (black arrows), and zigzag crumpled laminae (yellow arrow) in *C. cf. C. mammillatum* near the physical contacts of the two stromatoporoids. (4–9) Schematic drawing to illustrate the process of ecological interactions between two stromatoporoids in (1).

180x173mm (300 x 300 DPI)

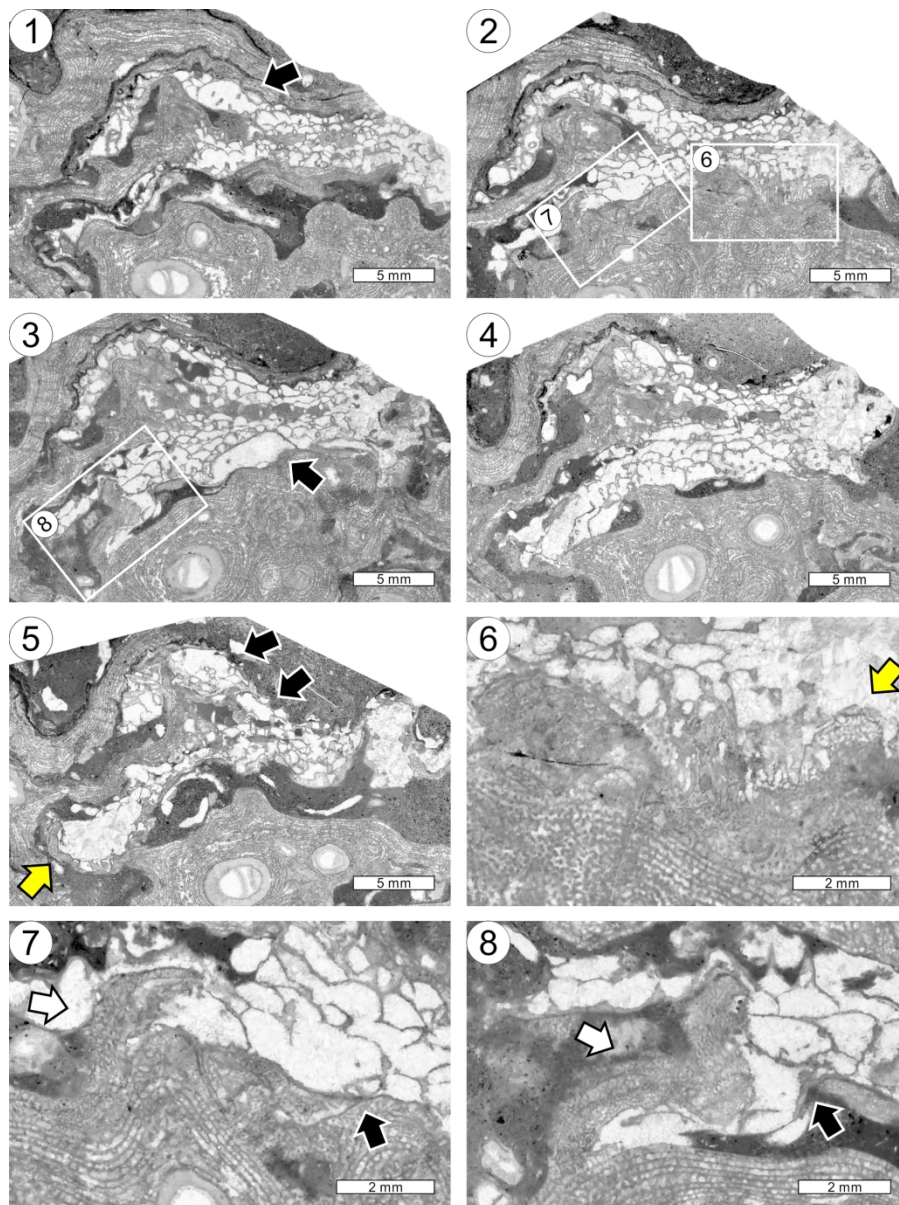


Figure 4. (1–5) Transverse serial sections showing distorted skeletal elements in *Labechia* sp. and *C. cf. C. mammillatum* during their ecological interactions, each interval ranging from 1.0 to 1.2 mm, respectively, exhibiting upward growth of the studied specimen, NIGP 169634-8-12. (6) Enlargement of the left rectangular area in (2). (7) Enlargement of the right rectangular area in (3). (8) Enlargement of the right rectangular area in (2). Space occupation of the laminae of *C. cf. C. mammillatum* is reflected by their skeletal distortions (white arrows in 7 and 8) in the cyst interspaces of *Labechia* sp. Large-sized and irregular-shaped cysts of *Labechia* sp. are indicated by black arrows, while crumpled laminae of *C. cf. C. mammillatum* are indicated by yellow arrows.

180x240mm (300 x 300 DPI)

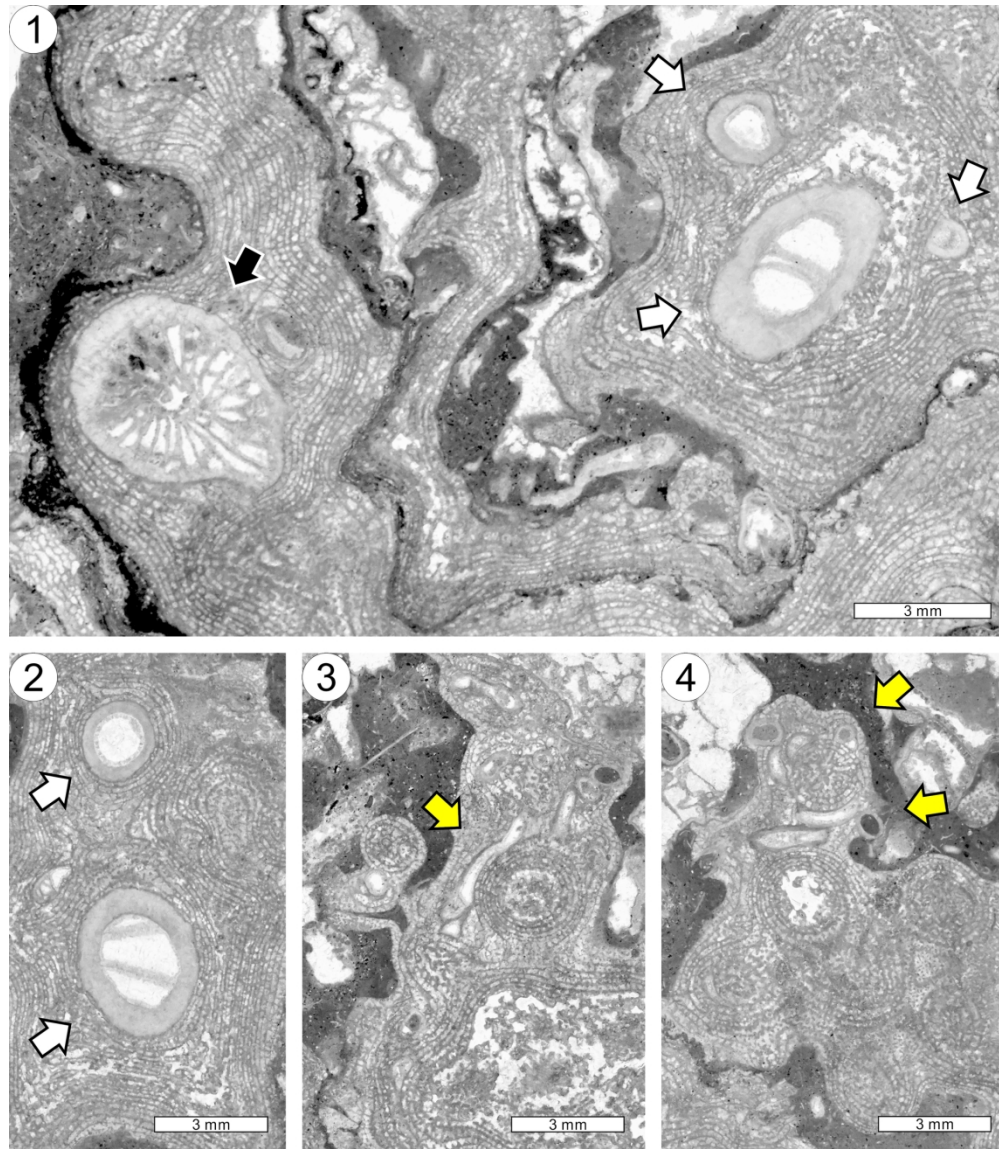


Figure 5. Thin section photographs of coral endobionts within the skeleton of *Clathrodictyon* cf. *C. mammillatum*. (1) Oblique-cut of three solitary rugose coral *Tryplasma* (white arrows) and a solitary rugose coral *Streptelasma* (black arrow) surrounded by *C. cf. C. mammillatum*, NIGP 169634-8. (2) Two solitary rugose coral *Tryplasma* (white arrows) near the mamelon column of *C. cf. C. mammillatum*, NIGP 169634-11. (3-4) Transverse views of mamelon columns of *C. cf. C. mammillatum* and the neighboring endobiont tabulate coral *Bajgolia* (yellow arrows). Note that no distortion of *C. cf. C. mammillatum* is observed near the contacts with diverse endobionts, NIGP 169634-7, 6, respectively.

180x205mm (300 x 300 DPI)

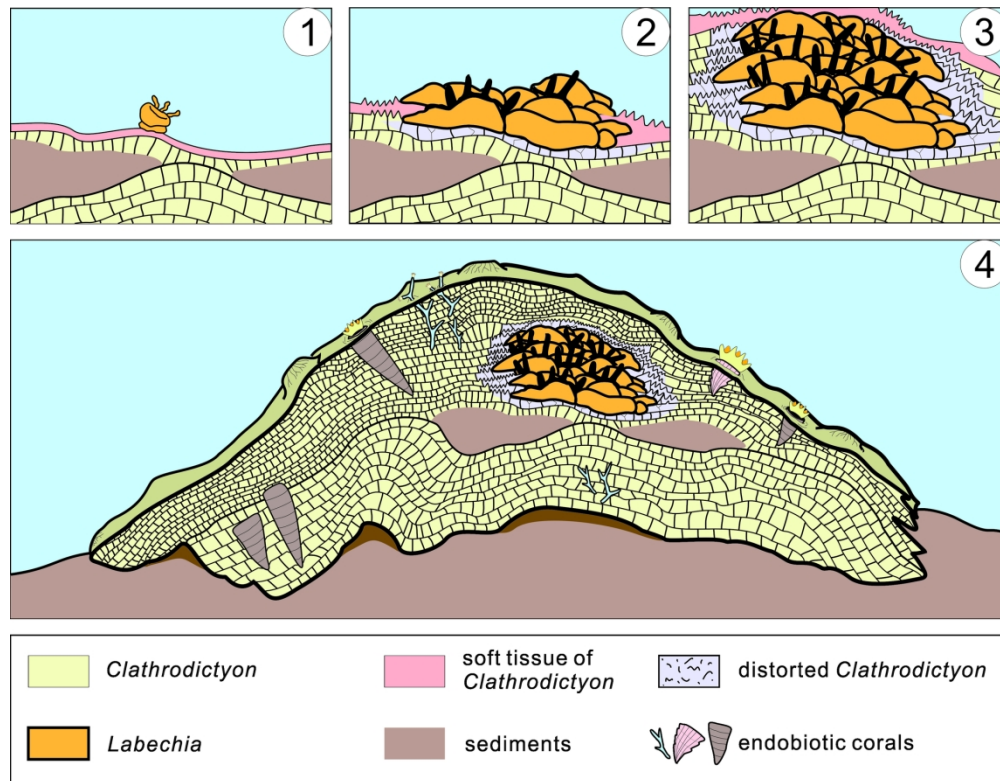


Figure 6. Schematic drawing to show the process of ecological interactions between two stromatoporoids. (1) Settlement of *Labechia* sp. on the growth surface of *Clathrodictyon*; (2) With the growth of *Labechia* sp., distorted skeleton of *C. cf. C. mammillatum* appears; (3) *Labechia* sp. is overgrown by *C. cf. C. mammillatum*; (4) Schematic drawing to illustrate the vertical view of *Clathrodictyon* and its endobionts including *Labechia* sp., rugose and tabulate corals.

180x140mm (300 x 300 DPI)